Synthesis of Ti matrix composites reinforced with TiC particles: thermodynamic equilibrium and change in microstructure

Jérôme Roger, Bruno Gardiola, J. Andrieux, Jean-Claude Viala, Olivier Dezellus

Journal of Materials Science (2016), DOI 10.1007/s10853-016-0677-y

Synthesis of Ti matrix composites reinforced with TiC particles: thermodynamic equilibrium and change in microstructure

Jérôme Roger[1,*], Bruno Gardiola[1], Jérôme Andrieux[1], Jean-Claude Viala[1], Olivier Dezellus[1]

[1] Université Claude Bernard LYON1, Laboratoire des Multimatériaux et Interfaces, UMR CNRS 5615, F-69622 Villeurbanne, France

[*] Author presently at Univ Bordeaux, CNRS, Lab Composites ThermoStruct, UMR 5801, F-33600 Pessac, France.

Abstract

The evolution of TiC reinforcement during the high-temperature consolidation step of a particulate-reinforced Ti matrix composite has been studied. A four-step scenario has been highlighted starting with the dissolution of the smallest particles to reach C saturation of the Ti matrix, followed by a change in the TiC stoichiometry from the initial $TiC_{0.96}$ composition to the equilibrium composition ($TiC_{0.57}$). This change in composition induces an increase in both the total mass fraction of reinforcement and the particle diameter. The diameter increase promotes contact between individual particles in the most reinforced domains and initiates an aggregation phenomenon that is responsible for the observed high growth rate of particles for heat treatment times shorter than 1h. Finally Ostwald ripening is responsible for the growth of particles for longer heat treatment times.

Keywords: Metal matrix composite; Titanium; Titanium carbide; Chemical change; Processing

1. Introduction

In the general context of structural lightening in the aerospace industry, Metal Matrix Composites (MMC) materials have attracted much interest over the past decades because of their high specific mechanical properties (relative to density) compared to existing metallic alloys. Of the fibers or particulate materials used as reinforcement for Ti-based composites, titanium carbide (TiC) has been widely investigated because of its excellent chemical compatibility with the matrix alloys [1–3]. Ti-TiC composites can be prepared by different routes although the most widely used is the classical powder metallurgy route [4, 5]. The nature of bonding at the matrix-reinforcement interface and the existence and extent of any reaction zone determine, to a large extent, the properties of the composite material.

From the binary Ti-C phase diagram (see Figure 1 - [6]), the expected interaction between a Ti-based matrix and commercial stoichiometric TiC particles, consists of the formation of a sub-stoichiometric form of the carbide according to reaction (1):

$$(1-x)TiC + x\,Ti \rightarrow TiC_{1-x}$$

Different studies have already reported experimental evidence of this trend towards thermodynamic equilibrium in the Ti-C binary system [7–9].

The aim of the present work is to report on the kinetics of the reaction path whereby a Ti-TiC composite material tends towards its thermodynamic equilibrium, and on the consequences of this trend on the microstructure and expected mechanical properties of the MMC material. Ti-TiC powder compacts were subjected to short-duration heat treatment at about 900°C and the reaction progress was monitored by removing the Ti-matrix by selective etching. The solid residu, containing the TiC particles was characterized by chemical analyses and X-ray diffraction (XRD). The present paper reports the results obtained after isothermal treatment and deals with the identification of the thermodynamic equilibrium and the change in Ti-TiC composite microstructure

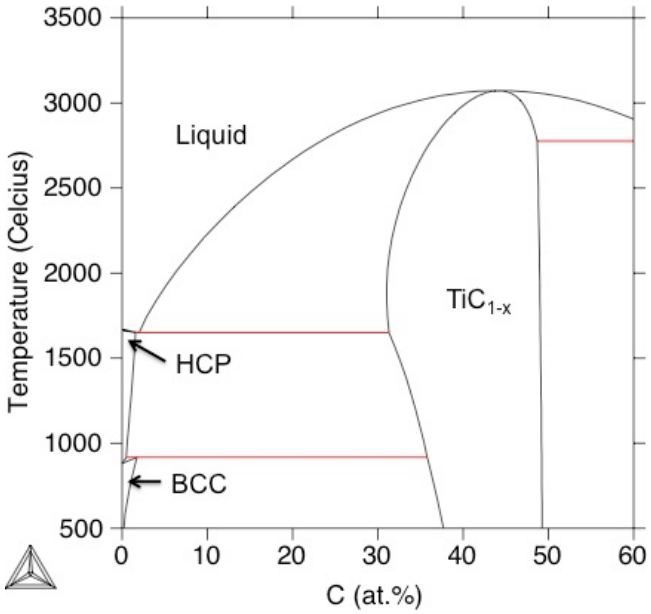

Figure 1: Calculated Ti-C binary phase diagram according to the assessment of Dumitrescu et al. [5].

2. Experimental procedures

2.1 Synthesis of samples

The Ti-15vol.%TiC (16.1wt.%) composite was synthesized from commercial TiC and Ti powders (see Tables 1 for their compositions) by the classical powder metallurgy route with a two-step procedure: high energy ball milling of the two starting materials (Ti and TiC powders) followed by extrusion of the ball-milled material after degassing and heat treatment for 1h at 920°C. More details on the experimental procedure, including the relative densities of materials, have already been reported [10]. Additional heat treatments at 920°C, both for longer and shorter heating times, were also performed. For long dwell times, from 2 to 450h, the extruded Ti-TiC composite (relative density higher than 99% [10]) was used as a starting material and the treatment was performed in a classical radiant furnace under purified Ar atmosphere in an alumina boat with a Ti getter in order to lower the oxygen partial pressure. For the shorter heat treatment time (from 1.5 to 20 minutes), dedicated small cylinders of powder compacts (7 mm diameter and 2 mm height) were prepared by cold unidirectional pressing with a typical load of 1200 MPa in a tungsten carbide (WC) matrix (relative density of about 80%). The pellets were then inserted under argon atmosphere in a graphite crucible. The graphite crucibles were degassed at 900°C under vacuum before each experiment and finally filled with Ar. Before insertion of the specimen sample, the crucible was filled with a layer of Ti powder that was used as a getter for gaseous impurities such as oxygen or nitrogen, and maintained in an Ar atmosphere. Finally, the prepared crucible was removed from the argon atmosphere just before the experiments and rapidly immersed in an aluminium-silicon (Al-Si) melt heated to the desired temperature (900°C in this study) by r.f. heating. Because of the inertial mass of the Al-Si melt (about 100g) compared to the mass of the graphite crucible (about 1g), rapid heating with a typical rate of about 400 K/s is ensured while a similar cooling rate is obtained by water quenching of the graphite crucible after removal from the Al-Si bath. With this procedure, the dwell time is optimized compared to the heating and cooling times allowing the investigation of short-duration experiments. In the present study, the dwell times are set between 1.5 min and 20 min.

	Element concentration (in mass %)						
	Ti	Al	V	Fe	C	O	N
Ti grade2 powder	Balance	-	-	0.0164	<0.10	0.16	<0.10

	Element concentration (in mass %)							
	Ti	Total C	N	O	Fe	Cr	V	Mo
	78.97	19.74	0.18	0.69	0.13	0.096	0.82	<0.05
TiC (starting powder)	Element concentration (ppm in mass) X-Ray fluorescence analysis of the impurities							
	Fe	Cr	V	Ni	Ca	Cu, Cl, K, Zn, S, Er, As		
	1200	118	170	116	77	traces		

Table 1. Chemical analysis of the Ti and TiC powder used as starting material (SCA CNRS Solaize)

2.4 Characterization of samples

The reaction mechanism was characterized by focusing on the change in structural and chemical properties of the carbide particles used as reinforcement.
Therefore, the first step of the characterization procedure involved selective etching in concentrated HF aqueous solution (60% in mass). However, since the origin of selectivity between the Ti matrix and the TiC particles is based on kinetics, it was necessary to moderate the etching rate. As a consequence, the sample was etched at low temperature, between -15°C and -5°C with small additions of composite material. In these experimental conditions, an average etching rate of about 0.25 g of composite per hour was observed. After etching, the sample was rinsed by removing 90% of the liquid and adding deionized water. When the remaining particles had settled, the rinsing/dilution procedure was repeated up to 10 times. Finally, the particles were dried under air, weighed and characterized by several techniques. It is clear that the whole extraction process induces a selective lost of the smallest particles of TiC either during etching, that is not perfectly selective, or during the rinsing procedure. However, by weighing carbide particles resulting from the dissolution of a standard sample synthesized in the laboratory with a perfectly known amount of TiC phase, it has been shown that more than 90% of the carbide is recovered after the extraction process.

X-ray diffraction (XRD) performed on a Panalytical XPert Pro MPD in Bragg-Brentano configuration was systematically used to characterize the structural changes in the carbide particles during the heat treatment. Cu Kα radiation was used and for sake of clarity in XRD patterns the Rachinger procedure was applied to remove the contribution of Cu $K\alpha_2$ radiation [11]. In order to ensure a high precision in the determination of the angular position of the

diffraction peaks, the carbide powder was dispersed as a thin film on a Si monocrystal (without any diffraction peak in the 10-110° angular range) and Si powder was also added as an internal reference. After correction of z-displacement by using the internal Si reference, the cell parameter of the TiC phase was determined from the 2θ peaks positions by a Pattern Matching method [12, 13]. The full-width at half maximum (FWHM) was evaluated with WINPLOTR software for (111), (200) and (022) reflections of the cubic carbide (located at 2θ ~ 36, 42 and 60° respectively) in order to calculate an average crystallite size using the Scherrer formula where $\beta = \beta_{observed} - \beta_{theo}$ is expressed in radians (with $\beta_{theo} = 0.04$):

$$T = 0.89\ \lambda / \beta.\cos\theta \qquad \text{(Equation 1)}$$

Oxygen, nitrogen and carbon contents of the extracted carbide particles were measured by an inert gas fusion instrument for nitrogen–oxygen determination (TC-300, LECO), and an infrared absorption carbon analyzer (EMIA-221V20K, Horiba), respectively. The absolute uncertainty associated with these methods is 0.5wt.% for oxygen and carbon and 0.3wt.% for nitrogen. Metallic elements were analyzed either by X-ray fluorescence or by atomic emission spectroscopy (ICP-AES). The presence of residual water in the extracted and dried carbide powder was evaluated using the Karl-Fisher analytical technique with a relative uncertainty of about 3-5%. Some characterization of TiC powders was also performed by Scanning Electron Microscopy on a Quanta FEI 250 FEG apparatus at the “Centre Technologique des Microstructures” at the University of Lyon 1.

3. Experimental Results

3.1 Starting TiC material

Figure 2a shows the morphology of the starting TiC powder observed by SEM. The frequency distribution of the maximum Feret diameter for a population of about 1500 particles is also presented in Figure 2a on the right-hand side of the SEM micrograph. The particle size distribution is clearly continuous as it ranges from 15-20 nm for the smallest to 7-10 µm for the biggest ones. Consequently, as the upper and lower limits of the size population cannot be detected using the same magnification during SEM characterization, it is difficult to build a complete histogram by image analysis. However, from these measurements the mean size can be estimated as being about 1 µm while the median value is about 0.7 µm.

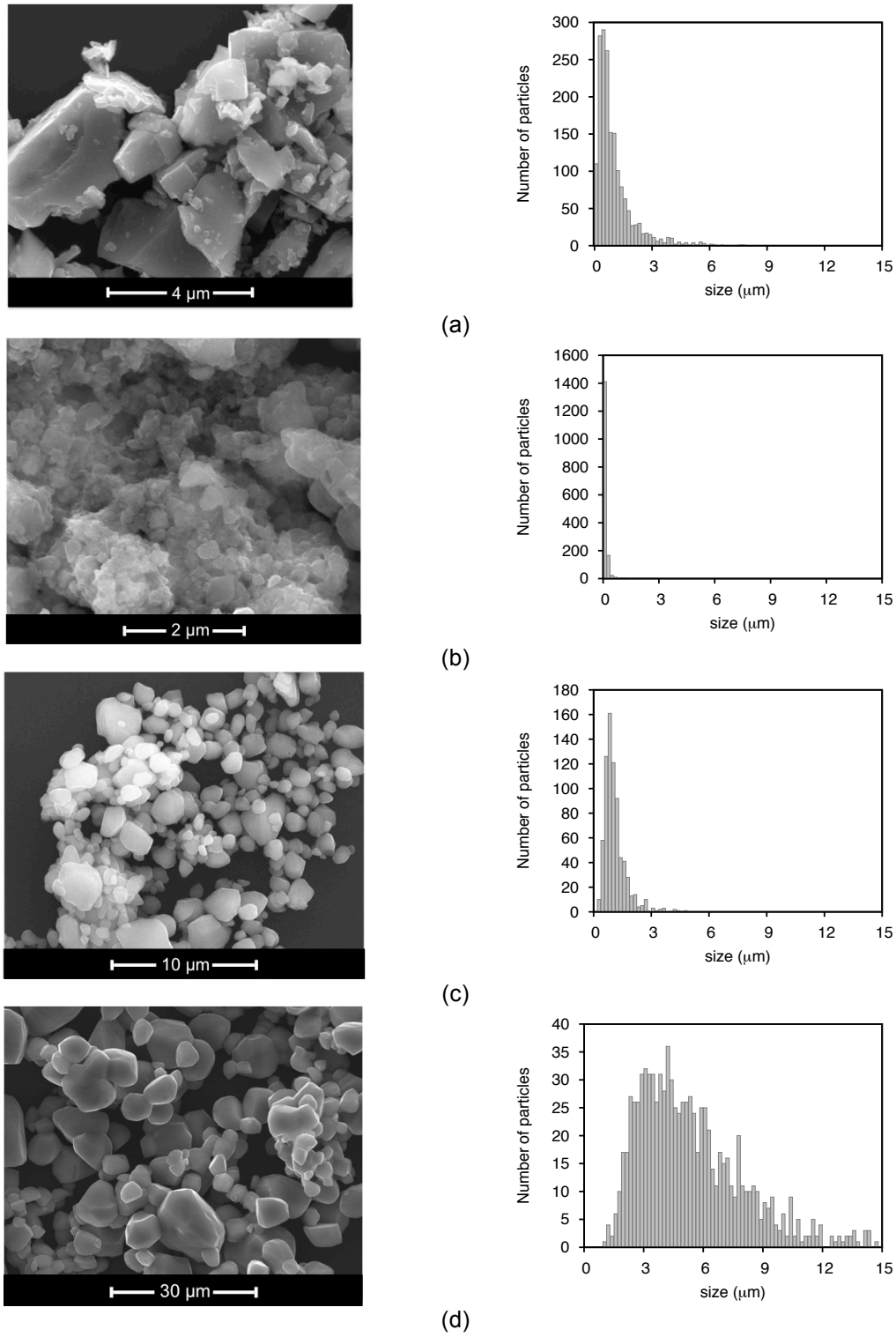

Figure 2: SEM micrograph and distribution of maximum Feret diameter of TiC powder particles obtained from SEM micrograph. (a) starting powder, (b) extracted from Ti matrix after the ball milling step, (c) extracted from Ti matrix after the consolidation step at 920°C

The pattern matching procedure [12] performed on the X-Ray pattern of titanium carbide (TiC) starting powder indicated a cell parameter of 0.43283(3) nm. According to the literature, this cell

parameter value corresponds to a nearly stoichiometric composition of the carbide [14]. This is in agreement with the C content determined by chemical analysis of the powder, i.e., about 19.74 wt.%C (49.5 at.%) (see Table 1). Consequently, the starting TiC powder has a nearly stoichiometric composition with a typical chemical formula $TiC_{0.96}$. It should be noted that the presence of particles smaller than 100 nm in the particle size distribution (see Figure 2a), induces a significant broadening of the base of diffraction peak (see Figure 3, "starting powder"). As a result, it is difficult to deduce the crystallite size either from the Scherrer formula or from the pattern matching procedure because of an existing continuum from nanometer to micron sized particles leading to a non-conventional peak shape.

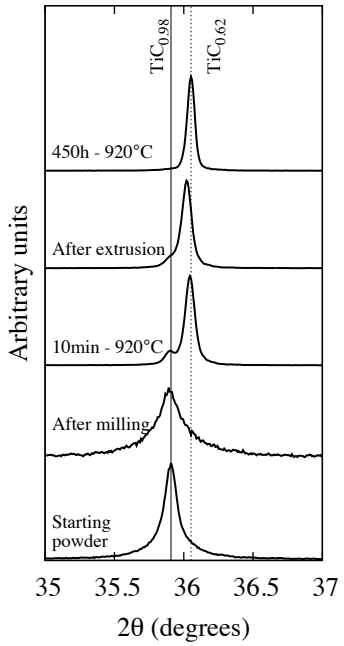

Figure 3: Details of the <111> X-ray diffraction peak shape obtained on: the starting TiC powder ; TiC extracted from the Ti matrix after the high-energy ball milling step and TiC extracted from the Ti matrix after 5 min and 450 h of heat treatment at 920°C. The intensity of each diffraction pattern is given in arbitrary units.

Finally, the chemical composition of the TiC starting powder was determined by several analysis techniques. The contents of the main elements as well as the impurities determined by X-ray fluorescence analysis are reported in Table 1. The total amount of carbon is about 19.7 wt.% (including an estimated 0.2 wt.% of free carbon) corresponding to a composition of the starting TiC powder that is nearly stoichiometric. More precisely, this composition is about $TiC_{0.96\pm0,01}$. The analyses have also shown the presence of nitrogen (0.2%), oxygen (0.7%), iron (0.1%), vanadium (0.08%) and other impurities with a typical content of less than 100ppm.

3.2 Ball-milled composite

Before the consolidation step performed by extrusion at 920°C, the Ti/TiC powder mixture is subjected to high-energy ball milling with the main objective being to reduce the size of the carbide particles significantly. This is confirmed by the analysis of SEM images obtained on the TiC particles after selective extraction from the Ti matrix, giving an average size of about 130 nm (see Figure 2b) compared to the mean size of 1 micrometer observed in the starting TiC powder, before ball milling (see Figure 2a). It should be noted that while the mean size is reduced by a factor of ten, some micrometer-sized particles are still present in the composite after ball milling. The reduction in size of the TiC particles is illustrated by the change in the X-ray diffraction pattern presented in Figure 3 showing a broadening of the diffraction peak.

3.3 Extruded composite

After the extrusion step characterized by heat treatment at 920°C, the composite material presents a characteristic duplex microstructure (see Figure 4) with fiber-like veins that are either unreinforced Ti matrix (light grey area on Figure 4) or reinforced composite (dark grey areas). Image analysis performed on Figure 4 leads to an estimation of the reinforced domains of about 40% of the analyzed surface. As a first approximation, it can therefore be considered that 40 vol.% of the composite consists in reinforced domains, containing almost all the TiC particles, while the remaining unreinforced domains represent 60 vol.%. As a consequence, whether the global amount of TiC particle is 15vol.%, the particles are not uniformly distributed with a typical 50vol.% amount in the reinforced domains. This microstructure results mainly from the heterogeneous dispersion of TiC particles inside the Ti matrix powder during the ball-milling step (duplex) and also from the consolidation process, i.e. extrusion (fiber-like veins). Note that heat treatment consists of 1h inside the furnace and therefore this time corresponds both to the heating step and the isothermal dwell. Concomitantly with the formation of this duplex microstructure, a major change in the particle morphology is also observed. First, the mean size increases from 130 nm after the milling step to about 1 µm after high-temperature treatment and extrusion. This size increase is associated with a significant narrowing of the size distribution around the mean size compared to the distribution of the starting powder (see Figure 2c).

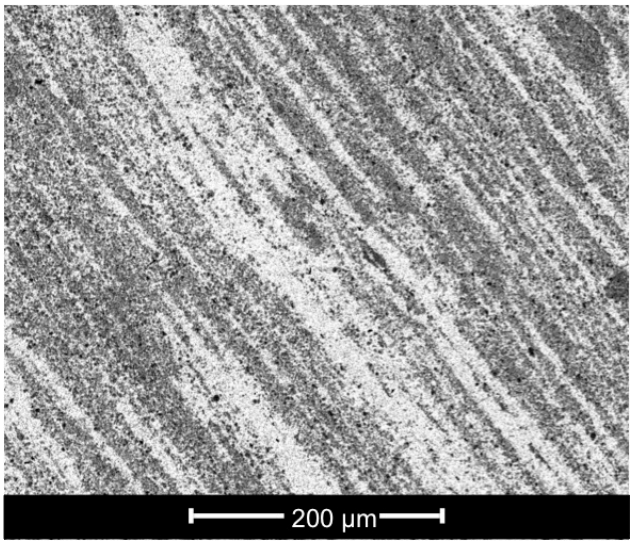

Figure 4: SEM micrograph of a Ti-15vol.%TiC sample after the consolidation step by extrusion at 920°C. The light grey fibers correspond to unreinforced Ti matrix coming from unreinforced powder particles elongated during the extrusion process.

A comparison of the TiC diffraction patterns obtained after extraction from the ball-milled and the extruded composite is shown in Figure 3 in case of the (111) reflection. It would appear firstly that, after heat treatment at 920°C, the diffraction peak is a convolution of two contributions: the less intense contribution corresponds to the angular position of the starting TiC powder ($TiC_{0.96}$) and will therefore be named in that which follows as the "residual contribution". Moreover, an additional and more intense contribution is also observed for higher 2θ values. This result is clear evidence of the formation during heat treatment at 920°C of a new TiC population characterized by a lower lattice parameter and therefore by a depletion in carbon leading to a non-stoichiometric carbide TiC_{1-x} [14]. It should also be noted that the FWHM characteristic of the diffraction peak of this new TiC_{1-x} population is significantly lower than that of the residual contribution, corresponding to a larger size of the coherent domains estimated by the Scherrer formula at around 200 nm.

The initial mass content in TiC of the composite material, before any treatment, is about 16.1wt.% whereas, after the consolidation step at 920°C, the carbide content is measured after

selective etching as being about 20wt.% (lower bound value). This mass increase is explained by the change in composition of the TiC phase from its initial $TiC_{0.96\pm0,01}$ composition toward its equilibrium composition with the Ti matrix according to reaction 1. This reaction leads to a conversion of the Ti matrix into a new population of sub-stoichiometric TiC_{1-x} population, and therefore to an increase of the weight fraction of TiC phase.

3.4 Thermodynamic equilibrium: 450h heat treatment at 920°C

A compact powder pellet of Ti-15vol.%TiC (16.1wt.%) was subjected to dedicated long-term (450h) heat treatment in a classical radiant furnace in order to clearly identify the thermodynamic equilibrium that tends to be established at 920°C. Figure 3 shows that a unique and well-crystallized population of TiC is observed with a cell parameter of 0.43153(5) nm. The residual amount of stoichiometric TiC determined by the full pattern matching procedure is about 0.5 wt.%. In that which follows, this residual content is considered to be negligible and without any significant influence on the chemical analysis of chemical composition of the extracted carbide powder. The chemical analysis performed on this extracted TiC powder gave about 12.5 wt.% (36.3 at.% - C/Ti = 0.57). This composition is reported on the Ti-C phase diagram (see Figure 5, filled triangle) and appears to be in good agreement with the accepted equilibrium composition. The set of combined values of cell parameter and carbon content is also reported on the so-called Storms curve in Figure 6 (filled square) and compared with all literature results [14–22].
Apparent disagreement observed in Figure 6 with literature results regarding the relation between lattice parameter and C/Ti ratio can be explained by the possible role of oxygen. Oxygen is a common impurity not only from the residual atmosphere but also from native oxide film of starting powders, it can substitute for carbon in the TiC lattice and promote a significant decrease in lattice parameter [19, 23, 24]. In the present study, the sub-stoichiometric form of TiC is obtained after reaction in a matrix of titanium and therefore in a low oxygen potential condition. This is confirmed by the low oxygen content (less than 1wt.%) determined by chemical analysis on the extracted TiC powder (see table 2). At the opposite, most of the literature results reporting on the lattice parameter for low C/Ti ratios do not contain any quantitative analysis of the oxygen content, while a lattice parameter value of 0.431 nm can either correspond to a $TiC_{0.6}$ or to a $TiC_{0.8}O_{0.2}$ composition [24]. As a consequence, lattice parameter of the literature data determined for low C/Ti ratios might be carefully considered. Finally, it can be conclude from this 450h heat treatment experiment at 920°C, that the Ti/TiC powder compact pellets tend towards a thermodynamic equilibrium corresponding to a sub-stoichiometric TiC composition with a carbon content of 12.5 wt.% (36.3 at.%, i.e. $TiC_{0.57}$) and a lattice parameter of 0.4153(5) nm.

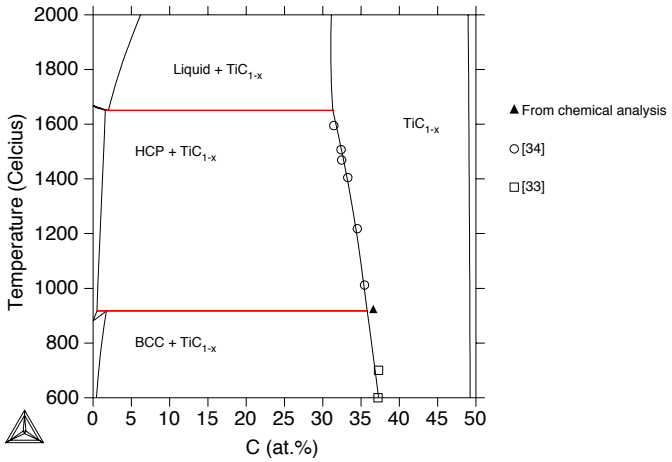

Figure 5: Variation in TiC lattice parameter in relation to C/Ti ratio. Three values are reported for a TiC powder extracted from a Ti/TiC powder pellet heat-treated for 450h at 920°C: from Rietveld refinement (filled blue circle), from mass increase (filled blue square) and from chemical analysis (filled blue triangle).

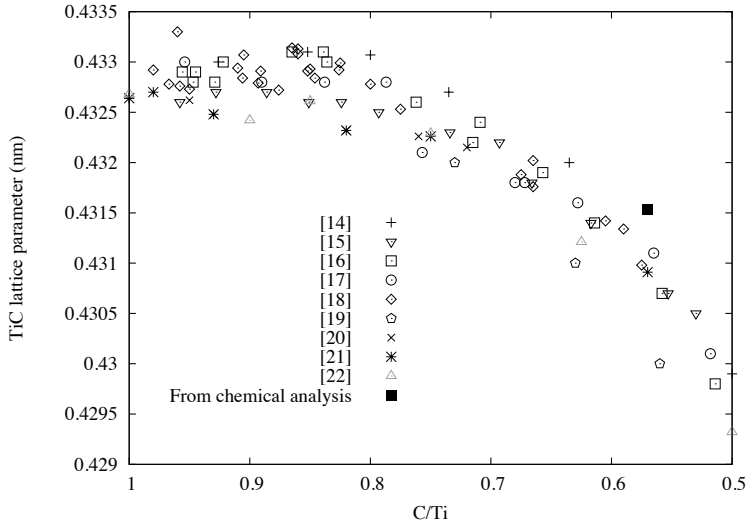

Figure 6: Visualization of compositions for a TiC powder extracted from a Ti/TiC powder pellet heat-treated for 450h at 920°C. Comparison with the calculated phase diagram according to the assessment of Dumitrescu et al. [5] and already published data on the extent of TiC_{1-x} phase [21,22].

Specimen	Content of elements (wt.%)			TiC_{1-x} stoichiometry according to the ratio C/C+Ti
	Ti	C	O	
Starting TiC powder	78.97	19.74	0,69	**$TiC_{0.98}$**
Consolidation step at 920°C	84.91%	13.23%	1.80%	**$TiC_{0.62}$**
Consolidation + 25h at 920°C	86.42%	12.77%	0.85%	**$TiC_{0.59}$**
Consolidation + 50 h at 920°C	86.48%	12.95%	1.35%	**$TiC_{0.60}$**
Consolidation + 100h at 920°C	86.14%	12.83%	1.74%	**$TiC_{0.59}$**
Consolidation + 450h at 920°C	85.94%	12.30%	0.70%	**$TiC_{0.57}$**

Table 2: Content of the elements Ti, C, O determined by chemical analysis on TiC powders extracted from Ti/ 15vol%TiC composite materials, after several heat treatments at 920°C, by selective acid dissolution of the Ti matrix.

3.5 The kinetics of the thermodynamic equilibrium trend

Once the starting TiC powder and its final equilibrium state have been well characterized, it is possible to study the kinetics of change in TiC powder during heat treatment at 920°C inside the Ti matrix. Two types of heat treatment were performed: medium-term heat treatments, from 25 to 100h, on the Ti-15vol.%TiC (16.1wt.%) composite after the extrusion consolidation step. These heat treatments can therefore be considered as additional treatments, after the consolidation step at 920°C for a dwell time of about 1h. The second type of heat treatment is a short-term heat treatment of Ti-15vol.%TiC (16.1wt.%) powder compacts (dwell time ranging from 1 to 20 minutes). These compacts were obtained by unidirectional pressing of the same starting materials but without any high temperature consolidation step prior to the treatment.

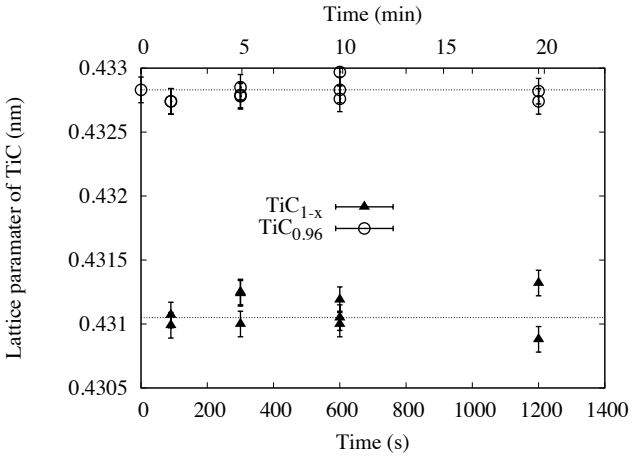

Figure 7: Variation in the relative content of respectively the initial stoichiometric TiC and the final substoichiometric $TiC_{0.57}$ as a function of heat treatment time. The values are determined by Rietveld refinement on the TiC powder extracted by acid etching from a Ti-15vol.%TiC compact after isothermal treatment at 920°C.

Quantitative phase analysis was performed by full pattern matching procedure (Rietveld refinement) [25, 26] of the diffraction patterns obtained after selective extraction of the TiC powder from the metallic matrix using BRASS software [27] and the assumptions of two TiC populations: the initial stoichiometric population ($TiC_{0.96}$) and the sub-stoichiometric population TiC_{1-x}. Figure 7 illustrates that the lattice parameters determined by the full pattern matching procedure for both the initial and the new sub-stoichiometric TiC_{1-x} populations, can be considered as being constants whatever the heat treatment time at 920°C and respectively equal to $a_{TiC0.96}$ = 0.4328(3) nm and a_{TiC1-x} = 0.4310(3) nm. As a consequence, each diffraction peak is considered as being the convolution of a contribution of the initial $TiC_{0.96}$ population (high lattice parameter), and the transformed TiC_{1-x} population (low lattice parameter). Figure 8 illustrates the result of Rietveld refinement procedure in case of TiC powder extracted from the Ti matrix after 10min at 920°C. As stated by the IUCR commission on Powder Diffraction the quality of Rietveld refinements is judged via a graphical examination of the observed and calculated diffraction data and the values of the Bragg R factor for each TiC population ($R_{Bragg\text{-}TiC0.96}$ = 4.72 and $R_{Bragg\text{-}TiC1\text{-}x}$ = 3.59) [28].

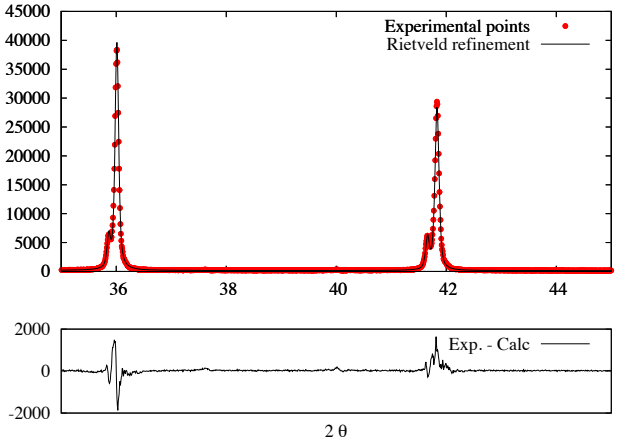

Figure 8: Variation in the size of coherent domains of the TiC powder extracted by acid etching from a Ti-15vol.%TiC compact after several heat treatment times at 920°C. The values are deduced by Rietveld refinement.

Finally, the amount of the two carbide populations is estimated from the Rietveld refinement and reported in Figure 9. Note that evolution of the new population of TiC_{1-x} (i.e. TiC_{1-x} in Figure 9) can be considered as a fraction-transformed plot of reaction 1. It should be noted that, for heat treatment times greater than 25h, no residual stoichiometric TiC is detected by XRD. The residual amount of the nominal composition of the carbide can therefore be considered to be less than 1wt.%, indicating that the conversion reaction, from the nominal stoichiometric composition to the composition in equilibrium with the Ti matrix, is almost complete. Secondly, it appears from Figure 9 that about 80% of the conversion has already occurred during the transient heating stage of the sample and the first 300s of dwell time at 920°C. Applying the Scherrer formula to the FWHM of the X-ray diffraction peaks, it is also possible to determine the size of coherent domains of the TiC_{1-x} particles after selective acid etching (see Figure 10). Note that for heat treatment times greater than 100h, the crystallite size becomes too large and does not lead to any significant broadening of the diffraction peak. A linear dependence of $<R_c^3>$ with time can be deduced between 1h and 100h that is in agreement with a growth mechanism of the crystallite dictated by the classical Ostwald ripening phenomenon limited by a diffusion step [29]. However, such a process is unable to explain the rapid growth of crystallite that is observed for short heat treatment times (shorter than 1h).

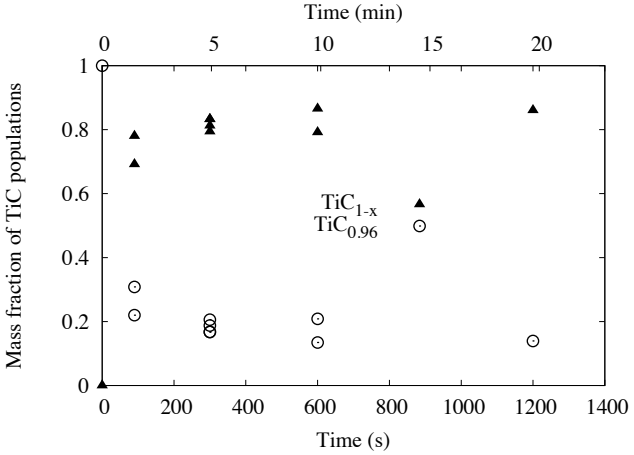

Figure 9: Variation in the size of coherent domains (R_c) to the power 3 of the TiC powder extracted from a Ti-15vol.%TiC compact as a function of heat treatment times at 920°C.

Additional information is obtained from SEM observations on the extracted particles. The mean diameter of the particles and their size distribution are evaluated after careful measurements on more than 1000 particles. Figure 2 displays the particle size distribution (PSD) obtained on starting TiC powder, the powder extracted from the composite after ball-milling, the powder extracted from the composite after extrusion and finally after an additional treatment of 450h at 920°C. To complete the trends qualitatively seen in Figure 2, some pertinent statistical parameters such as the mean, the coefficient of Skewness and the coefficient of excess Kurtosis are reported in Table 3. Skewness is a measure of the symmetry of the distribution; a normal, Gaussian distribution has a Skewness value of 0. The excess Kurtosis can be used to compare the peakedness of a distribution with the Gaussian distribution: excess Kurtosis is equal to 0 for Gaussian, whereas a more peaked distribution with an excess density in the tails has a positive value of excess Kurtosis [30]. It appears firstly that the most important change in the PSD shape is induced by the milling process with a significant reduction of the mean and high values of the Skewness and excess Kurtosis parameters. These unusually high values correspond to a peaked distribution with a very extended right tail caused by the existence of residual initial particles unaffected by the milling process (several microns in size). After only 90s heat treatment at 920°C, the shape of the size distribution is again strongly modified, much less peaked but still skewed with a pronounced right-hand tail. Finally, the distribution tends to approach a stable shape at longer heat treatment times that is characterized by an increase of the mean size and a decrease of the values for excess Kurtosis and Skewness.

Sample	Mean (μm)	Median (μm)	Excess Kurtosis	Skewness
Starting material	1.013	0.969	8.42	2.53
After ball milling	0.128	0.166	110.00	8.96
About 1h (consolidation step)	1.103	0.583	7.44	2.21
TiC powder extracted from Ti matrix after several heat treatment at 920°C				
t = 1 min 30s	0.552	0.303	6.15	2.00
t = 5 min	0.878	0.459	9.53	2.31
Consolidation + 25h	2.568	1.110	6.55	1.69
Consolidation + 100h	3.150	1.523	2.21	1.27
Consolidation + 454h	5.437	2.750	1.53	1.17

Table 3: Data from the experimental particle size distribution for the TiC powder extracted from the Ti matrix at different step of the synthesis procedure of Ti-15vol.%TiC composite and after different heat treatment times at 920°C.

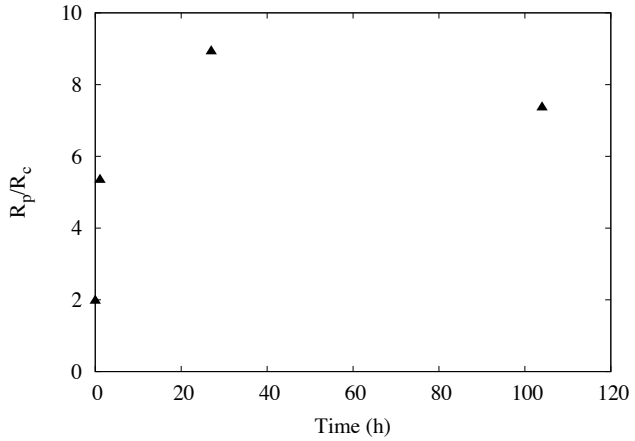

Figure 11: Change in the ratio between the mean size of particles (R_p) and coherent domains (R_c) of the TiC powder extracted by acid etching from a Ti-15vol.%TiC compact as a function of heat treatment times at 920°C.

Figure 11 shows the change in the ratio between the mean radius of the particles and the mean radius of the crystallite as a function of heat treatment time at 920°C. While the ratio is close to one after the milling step, indicating that most of the particles are single crystallite particles, the ratio increases sharply during the first hour of treatment at 920°C tending to a value of about 7 that remains constant during further heat treatment. This change means that, during heat treatment at 920°C, the TiC particles tend to be more polycrystalline, an observation that is not compatible with a growth mechanism dictated by Ostwald ripening.

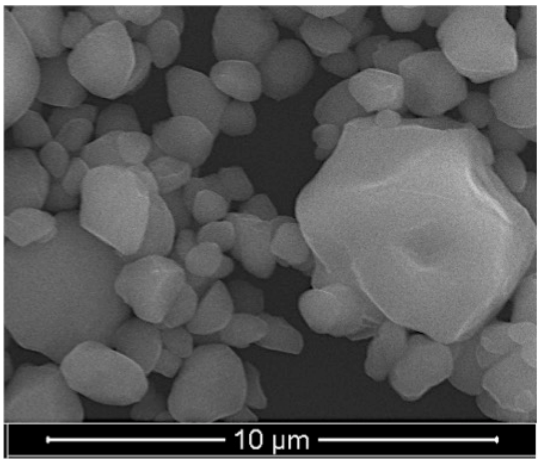

Figure 12: SEM micrograph of TiC particles extracted from Ti matrix of a Ti-15vol.%TiC composite after 100 h heat treatment at 920°C. An agglomerate of individual particles is visible in the bottom right-hand corner.

The SEM micrograph presented on Figure 12 illustrates an aggregation phenomenon of sub-micronic TiC particles to form larger agglomerates of particles that are finally considered to be single globular particles during the counting procedure. The change in composition of TiC particles according to reaction 1 induces an increase of their volume by a factor 1.66; leading to an increase of the volume fraction of particles. Moreover, because of the heterogeneous dispersion of TiC particles in 40% of the MMC volume (see Figure 4 and section 3.3), the volume fraction of reinforcement in the reinforced domains can be estimated as being about 50vol.% after conversion of the carbide from $TiC_{0.96}$ to $TiC_{0.57}$. At such high volume fraction the possibility of encounters of two particles is very high, leading firstly to their aggregation and next to their coalescence [31]. As a result, the growth phenomenon of particles is not only due to Ostwald ripening but also to the agglomeration and coalescence of small particles. The latter growth mechanism, by agglomeration, is clearly predominant for the shorter heat treatment times, less than 1h, and could explain the rapid growth of crystallite that is observed for short heat treatment times (see Figure 8), before Ostwald ripening becomes the main growth mechanism.

4. Discussion

Based on the experimental results, a detailed scenario is presented of the chemical interactions occurring between the Ti matrix and TiC particles during the high-temperature step of a metal matrix composite synthesis. Moreover, those chemical exchanges have major consequences on the composite microstructure and subsequently on the expected mechanical properties.

The first step of interaction consists of the saturation of the Ti matrix in carbon coming from the dissolution of some TiC particles. According to the phase equilibria in the Ti-C binary system [6], the solubility of C in the cubic form of titanium – β-Ti – at 920°C is about 0.5 at.% (0.13 wt.%). Therefore, considering that the initial C content is about 0.1at.% (see table 1), saturation of the Ti matrix of a 15vol.%TiC (16.1wt.%) composite induces the dissolution of about 1% of the TiC phase. However, during the heating procedure, maximum solubility is obtained in α-Ti when reaching its peritectic invariant decomposition at 915°C and is about 4 times greater (0.4 wt.%), thus leading to the expected dissolution of 8% of the initial amount of TiC particles. Despite the fact that this dissolution process is reversible during the cooling process, it has major consequences as the dissolution affects the smallest particles first of all.

After the transitory dissolution of TiC, the second step that has been directly observed is the change in TiC stoichiometry from its initial non-equilibrium composition $TiC_{0.96}$ to the measured equilibrium value of $TiC_{0.57}$. As this change is due to reaction 1, it is associated with an increase in the amount of TiC and, more precisely, with an increase in the volumetric amount by a factor of 1.66. Assuming spherical particles, this increase is associated with a diameter increase by a factor of 1.18 that is well below the factor of 8 observed during the consolidation step by

extrusion at 920°C. Moreover, it has been shown that the dispersion of TiC particles inside the Ti matrix is heterogeneous: the ball milling process leads to a duplex microstructure with Ti particles free of reinforcement surrounded by Ti composite particles with a typical amount of TiC that is about 40 vol.%. Consequently, with such a high volumetric amount, the increase in particle diameter due to the change in composition toward equilibrium, induces locally some contacts between particles followed by the formation of aggregates of particles. During the heat treatment, these aggregates coalesce and grow to form large globular particles in which the initial individual TiC particles cannot be discriminated. This phenomenon, already observed in the literature [32], is the only one that can explain the huge rate of growth (a factor of ten) observed during the first hour of heat treatment at 920°C.
Finally, once the Ti matrix is saturated in carbon (after step 1), Ostwald ripening occurs, leading to the selective growth of the bigger TiC particles and associated with the disappearance of the smallest ones. This ripening mechanism is never pure: it is accompanied by a change in stoichiometry for very short times and aggregation with volume expansion and bonding of small particles for intermediate times.

5. Conclusion

The trend toward equilibrium of a Ti-TiC metal matrix composite synthesized by a powder metallurgy route was studied by following the change in the TiC particles after selective extraction from the metallic matrix at different steps of the synthesis procedure. Moreover, additional heat treatments were performed to clearly identify the thermodynamic equilibrium and highlight the mechanisms responsible for the kinetics of the change process.
Three different mechanisms were identified as being responsible for the change in TiC particles:

- The first is a change in composition from the initial stoichiometric value at the Ti-rich boundary in order to achieve thermodynamic equilibrium between matrix and reinforcement. This phenomenon is associated with dissolution of the smallest TiC particles followed by a significant increase in remaining particles mean diameter.
- The diameter increase, associated with an heterogeneous distribution of TiC particles in the composite, leads to the initiation of an aggregation phenomenon responsible for the fast growth rate (by a factor of 8) that was observed for the apparent particle size during the consolidation step at 920°C.
- Finally, the classical Ostwald ripening mechanism was observed to be active in order to explain the growth of TiC particles, mainly for long-term heat treatments.

One of the most striking results is the high rate of change of the first process corresponding to the tendency of TiC stoichiometry to reach its equilibrium composition with the Ti matrix. Various characterization methods clearly indicate that most of the change is achieved after only a few tenths of seconds at 920°C. Additional characterizations of the Ti-TiC composite trend during the two first steps of the scenario (dissolution and modification of stoichiometry) were performed in-situ by X-ray synchrotron diffraction and are presented in an incoming paper.

Finally, as no new phases are formed, the chemical exchanges that occur between a Ti matrix and TiC reinforcing particles can be considered to be slight modifications (adjustments of composition) in order to achieve the thermodynamic equilibrium conditions. However, they have major consequences on the powder metallurgy process and it is expected that there will also be consequences on the mechanical properties:

- Growth rate of TiC particles is so fast that a mean particle size greater than 1 μm will be systematically obtained after the high temperature consolidation step, whatever is the particles size distribution obtained by the ball-milling step.
- Heterogeneous dispersion and aggregation of TiC particles can lead to local embrittlement of the reinforced zone of the composite.

These phenomena have to be taken into account in order to design a process for the synthesis of an optimized Ti-TiC metal matrix composite by the powder metallurgy route.

Acknowledgements
This work was conducted in the framework of the COMETTi project sponsored by the French national research agency (ANR) under the reference ANR-09-MAPR-0021. The authors wish to thank the “Centre Technologique des Microstructures” (CTμ, http://microscopies.univ-lyon1.fr)

for help and advice during the SEM observations and the ‘‘Service Central d’Analyse, SCA, CNRS’’, and particularly P. James and L. Ayouni, for chemical analyses.

Conflict of Interest: The authors declare that they have no conflict of interest

References

1. Clyne TW, Withers PJ (1993) An introduction to Metal Matrix Composites. Cambridge University Press, Cambridge

2. Lindroos VK, Talvitie MJ (1995) Recent advances in metal matrix composites. Journal of Materials Processing Technology 53:273–284. doi: 10.1016/0924-0136(95)01985-N

3. Miracle DB (2005) Metal matrix composites – From science to technological significance. Composites Science and Technology 65:2526–2540. doi: 10.1016/j.compscitech.2005.05.027

4. Liu Y, Chen LF, Tang HP, et al (2006) Design of powder metallurgy titanium alloys and composites. Materials Science and Engineering: A 418:25–35. doi: 10.1016/j.msea.2005.10.057

5. Kondoh K (2015) Titanium metal matrix composites by powder metallurgy (PM) routes. In: Titanium Powder Metallurgy. Elsevier, pp 277–297

6. Dumitrescu LFS, Hillert M, Sundman B (1999) A reassessment of Ti-C-N based on a critical review of available assessments of Ti-N and Ti-C. Zeitschrift fur Metallkunde 90:534–541.

7. Wanjara P, Drew RAL, Root J, Yue S (2000) Evidence for stable stoichiometric Ti2C at the interface in TiC particulate reinforced Ti alloy composites. Acta Materialia 48:1443–1450. doi: 10.1016/S1359-6454(99)00453-X

8. Quinn C j., Kohlstedt D l. (1984) Solid-State Reaction Between Titanium Carbide and Titanium Metal. Journal of the American Ceramic Society 67:305–310. doi: 10.1111/j.1151-2916.1984.tb19527.x

9. Erlin Z, Songyan Z, Zhaojun Z (2000) Microstructure of XDTM Ti-6Al/TiC composites. Journal of Materials Science 35:5989–5994. doi: 10.1023/A:1026794810924

10. Fruhauf JB, Roger J, Dezellus O, et al (2012) Microstructural and mechanical comparison of Ti + 15%TiCp composites prepared by free sintering, HIP and extrusion. Materials Science and Engineering: A 554:22–32. doi: 10.1016/j.msea.2012.05.096

11. Rachinger WA (1948) A Correction for the α 1 α 2 Doublet in the Measurement of Widths of X-ray Diffraction Lines. J Sci Instrum 25:254. doi: 10.1088/0950-7671/25/7/125

12. Le Bail A (2005) Whole powder pattern decomposition methods and applications: A retrospection. Powder Diffr 20:316–326. doi: 10.1154/1.2135315

13. Louer D (1998) Advances in Powder Diffraction Analysis. Acta Crystallographica Section A 54:922–933.

14. Storms EK (1967) The refractory carbides. Academic Press, New York - London

15. Bittner H, Goretzki H (1962) Magnetische Untersuchungen Der Carbide Tic, Zrc, Hfc, Vc, Nbc Und Tac. Mon Chem 93:1000-. doi: 10.1007/BF00905899

16. Norton JT, Lewis RK (1963) Properties of non-stoichiometric metallic carbides. Advanced Metals Research Corp, Somerville, Massachusetts

17. Rudy E, Bruckl C, Harmond DP (1965) Ternary phase equilibria in transition metal-boron-carbon-silicon systems. Air Force Materials Laboratory , Research and Technology Division

18. Ramqvist L (1968) Variation of Lattice Parameter and Hardness with Carbon Content of Group 4 B Metal Carbides. Jernkontorets Annaler 152:517.

19. Vicens J, Chermant JL (1972) Contribution to study of system Titanium-Carbon-Oxygen. Revue de Chimie Minérale 9:557–567.

20. Kiparisov SS, Narva VK, Kolupaeva SY (1975) Effect of titanium carbide composition on the properties of titanium carbide-steel materials. Poroshk Metall 41–4.

21. Frage N, Levin L, Manor E, et al (1996) Iron-titanium-carbon system. II. Microstructure of titanium carbide (TiCx) of various stoichiometries infiltrated with iron-carbon alloy. Scripta Materialia 35:799–803. doi: 10.1016/1359-6462(96)00230-8

22. Fernandes JC, Anjinho C, Amaral PM, et al (2003) Characterisation of solar-synthesised TiCx (x=0.50, 0.625, 0.75, 0.85, 0.90 and 1.0) by X-ray diffraction, density and Vickers microhardness. Mater Chem Phys 77:711–718.

23. Nishimura H, Kimura H (1956) Titanium-oxygen-carbon system. IV. Nippon Kinzoku Gakkaishi 20:589–592.

24. Neumann G, Ettmayer P, Kieffer R (1972) System TiC-TiN-TiO. Monatshefte für Chemie 103:1130–1137.

25. Bish DL, Howard SA (1988) Quantitative phase analysis using the Rietveld method. Journal of Applied Crystallography 21:86–91.

26. León-Reina L, García-Maté M, Álvarez-Pinazo G, et al (2016) Accuracy in Rietveld quantitative phase analysis: a comparative study of strictly monochromatic Mo and Cu radiations. Journal of Applied Crystallography 49:722–735. doi: 10.1107/S1600576716003873

27. Burzlaff H, Hountas A (1982) Computer program for the derivation of symmetry operations from the space-group symbols. Journal of Applied Crystallography 15:464–467. doi: 10.1107/S0021889882012382

28. McCusker LB, Von Dreele RB, Cox DE, et al (1999) Rietveld refinement guidelines. Journal of Applied Crystallography 32:36–50. doi: 10.1107/S0021889898009856

29. Baldan A (2002) Review Progress in Ostwald ripening theories and their applications to nickel-base superalloys - Part I: Ostwald ripening theories. J Mater Sci 37:2171–2202. doi: 10.1023/A:1015388912729

30. MacKay RA, Nathal MV (1990) γ′ coarsening in high volume fraction nickel-base alloys. Acta Metallurgica et Materialia 38:993–1005. doi: 10.1016/0956-7151(90)90171-C

31. Jayanth CS, Nash P (1989) Factors affecting particle-coarsening kinetics and size distribution. Journal of Materials Science 24:3041–3052. doi: 10.1007/BF01139016

32. Kim Y-J, Chung H, Kang S-JL (2001) In situ formation of titanium carbide in titanium powder compacts by gas–solid reaction. Composites Part A: Applied Science and Manufacturing 32:731–738. doi: 10.1016/S1359-835X(99)00092-5

33. Cadoff I, Nielsen JP (1953) Titanium-carbon phase diagram. J Met 5:248–52.

34. van Loo FJJ, Bastin GF (1989) On the diffusion of carbon in titanium carbide. MTA 20:403–411. doi: 10.1007/BF02653919

FIGURES CAPTIONS

Figure 1: Calculated Ti-C binary phase diagram according to the assessment of Dumitrescu et al. [6].

Figure 2: SEM micrograph and distribution of maximum Feret diameter of TiC powder particles obtained from SEM micrograph. (a) starting powder, (b) extracted from Ti matrix after the ball milling step, (c) extracted from Ti matrix after the consolidation step at 920°C, (d) extracted from Ti matrix after additional time at 920°C (454h).

Figure 3: Details of the (111) X-ray diffraction peak shape obtained on: the starting TiC powder ; TiC extracted from the Ti matrix after the high-energy ball milling step and TiC extracted from the Ti matrix after 5 min and 450 h of heat treatment at 920°C. The intensity of each diffraction pattern is given in arbitrary units. Note that Cu $K\alpha_2$ contribution has been removed by Rachinger procedure [11].

Figure 4: SEM micrograph of a Ti-15vol.%TiC (16.1wt.%) sample after the consolidation step by extrusion at 920°C. The light grey fibers correspond to unreinforced Ti matrix coming from unreinforced powder particles elongated during the extrusion process.

Figure 5: Visualization of composition for a TiC powder extracted from a Ti/TiC powder pellet heat-treated for 450h at 920°C. Comparison with the calculated phase diagram according to the assessment of Dumitrescu et al. [6] and already published data on the extent of TiC_{1-x} phase [33, 34].

Figure 6: Variation in TiC lattice parameter in relation to C/Ti ratio. Present study reports one point for a TiC powder extracted from a Ti/TiC powder pellet heat-treated for 450h at 920°C: lattice parameter is obtained from Rietveld refinement while the composition results from chemical analysis.

Figure 7: Variation in the lattice parameters of respectively the initial stoichiometric TiC and the final substoichiometric $TiC_{0.57}$ populations as a function of heat treatment time. The values are determined by pattern matching performed on the TiC powder extracted by acid etching from a Ti-15vol.%TiC (16.1wt.%) compact after isothermal treatment at 920°C.

Figure 8: Observed and calculated diffraction pattern between of TiC powder extracted from Ti matrix after 10min heat treatment at 920°C. The lower panel graph shows the difference (Observed-Calculated). Diffraction pattern is limited to an expanded range between 35º and 45º highlighting the two main diffraction peaks of TiC structure. Note that Cu $K\alpha_2$ contribution has been removed by Rachinger procedure [11].

Figure 9: Variation in the relative content of respectively the initial stoichiometric TiC and the final substoichiometric $TiC_{0.57}$ as a function of heat treatment time. The values are determined by Rietveld refinement on the TiC powder extracted by acid etching from a Ti-15vol.%TiC (16.1wt.%) compact after isothermal treatment at 920°C.

Figure 10: Variation in the size of coherent domains of the TiC powder extracted by acid etching from a Ti-15vol.%TiC (16.1wt.%) compact after several heat treatment times at 920°C. The values are deduced by Rietveld refinement.

Figure 11: Change in the ratio between the mean size of particles (R_p) and coherent domains (R_c) of the TiC powder extracted by acid etching from a Ti-15vol.%TiC (16.1wt.%) compact as a function of heat treatment times at 920°C.

Figure 12: SEM micrograph of TiC particles extracted from Ti matrix of a Ti-15vol.%TiC (16.1wt.%) composite after 100 h heat treatment at 920°C. An agglomerate of individual particles is visible in the bottom right-hand corner.